December 22, 2019

Highlights of top quark physics at ATLAS

Roman Lysák
on behalf of the ATLAS collaboration[1]

Institute of Physics of the Czech Academy of Sciences,
Prague, Czech Republic

This contribution gives an overview of the most recent top quark measurements performed in LHC proton-proton collisions with the ATLAS detector, covering measurements of inclusive and differential cross-sections of top quark pair and single top quark production, measurements of the production of top quarks in association with electroweak gauge bosons or additional jets, precise measurements of the top quark mass and measurements of other top quark properties, such as the charge asymmetry of the top quark pair. Searches for flavour-changing neutral currents in the top quark sector are also discussed.

ATL-PHYS-PROC-2019-164
23 December 2019

PRESENTED AT

11^{th} High-Energy Physics International Conference
Antananarivo, Madagascar, October 14–19, 2019

1 Introduction

The fact that the top quark is much heavier than the other quarks or the leptons and that its mass is close to the electroweak (EWK) symmetry breaking scale makes the top quark special. This not only allows precision tests of the Standard Model (SM) at the large energy scale but also searches for physics beyond the SM (BSM).

Overall, around 160 millions of top quark events have been produced by LHC proton-proton collisions in the ATLAS experiment [1]. This much data allow precise inclusive and differential measurements of the production and properties of the top quark. Moreover, it is possible to search for the rare top quark production and new phenomena in the top quark sector.

The top quark is produced dominantly as top–antitop quark ($t\bar{t}$) pairs via the strong interaction. The single top quark production is possible via the electroweak interaction. Since the top quark decays mostly ($> 99\%$) as $t \to Wb$, the top quark decay chain is determined by the W boson leptonic ($W \to l\nu$) or hadronic ($W \to qq'$) decay. Most of the measurements presented here are performed in the top-quark pair dilepton ($t\bar{t} \to W^+bW^-\bar{b} \to l^+\nu bl^-\bar{\nu}\bar{b}$) or lepton+jets channel ($t\bar{t} \to WWb\bar{b} \to l\nu qq'b\bar{b}$).

In the following, only the latest ATLAS top quark measurements performed during the last year are presented. The measurements are performed at the center-of-mass energy $\sqrt{s} = 13$ TeV unless otherwise stated.

2 Inclusive and differential cross-sections

The measurement of inclusive $t\bar{t}$ or single top quark cross-section provides a basic test of SM in the top quark sector. The inclusive $t\bar{t}$ cross-section has been measured in both the dilepton and lepton+jets channels. In the dilepton channel [2], the events with one and two b-tagged jets* are counted, see Fig. 1 (left). The measured inclusive cross-section is $\sigma = 826.4 \pm 3.6$ (stat.) ± 11.5 (syst.) ± 15.7 (lumi.) ± 1.9 (beam) pb. In the lepton+jets channel [3], the fit to various distributions having a small sensitivity to the $t\bar{t}$ modeling is performed. The example of one such distribution is in Fig. 1 (right). The measured inclusive cross-section is $\sigma = 830.4 \pm 0.4$ (stat.)$^{+38.2}_{-37.0}$ (syst.) pb. Both measurements are very precise, especially the one in dilepton channel with an overall uncertainty of 2.4%, and are in excellent agreement with the latest theoretical prediction $\sigma = 832^{+20}_{-29}$ (scale) ± 35 (PDF + α_s) pb calculated at next-to-next-to-leading order (NNLO) in perturbative quantum chromodynamics (QCD), including soft-gluon resummation at next-to-next-to-leading-log order (NNLL) [4, and references therein].

The EWK single-top quark production is possible via various production channels: the t-channel (∼75% at LHC), the tW-channel (∼20%) and the s-channel (∼5%). ATLAS and CMS collaborations combined their individual measurements for each production channel at both LHC Run 1 center-of-mass energies of interactions, $\sqrt{s} = 7$ TeV and $\sqrt{s} = 8$ TeV [5]. All individual results and the combinations are summarized in Fig. 2 and are consistent with predictions. The uncertainty is 7%, 16% and 30% for the measurement at $\sqrt{s} = 8$ TeV in the t-, tW- and s-channel, respectively. This is still

*b-tagged jets are collimated spray of particles, jets, identified as those containing b-hadrons

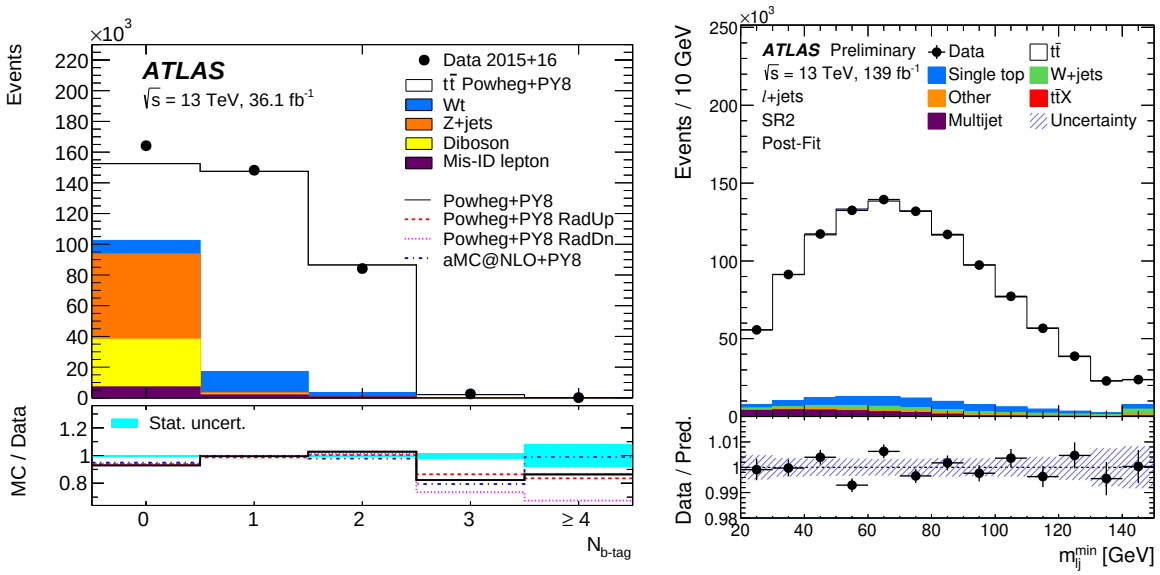

Figure 1: The distribution of the number of b-tagged jets in selected dilepton events (left) [2]. The post-fit distribution for the minimal invariant mass over all lepton-jet pairs, m_{lj}^{min}, (right) [3].

worse compared to the precision in the theoretical calculations which are in the range of 4–8% [5, and references therein].

The differential cross-section measurements provide a more detailed test of the top quark production compared to the inclusive measurements while improving the simula-

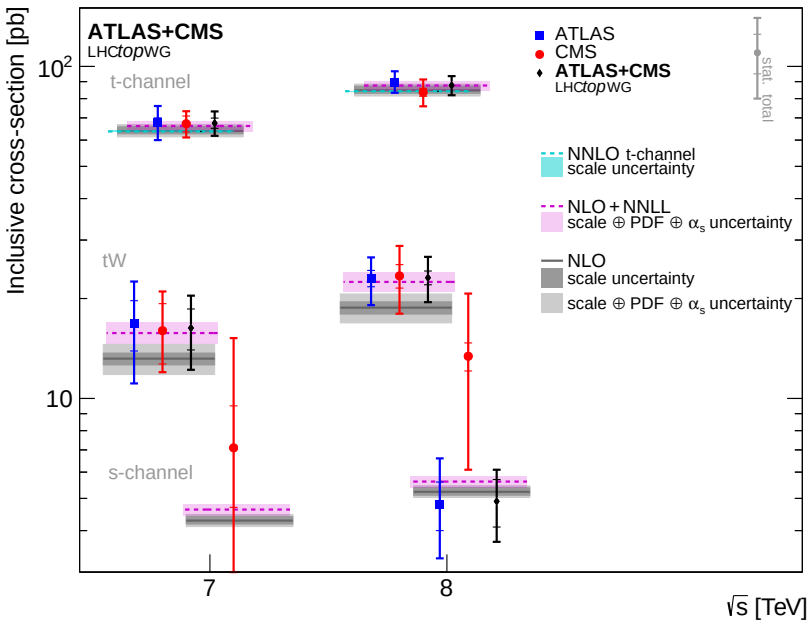

Figure 2: Single top quark cross-section measurements performed by ATLAS and CMS, together with the combined results [5].

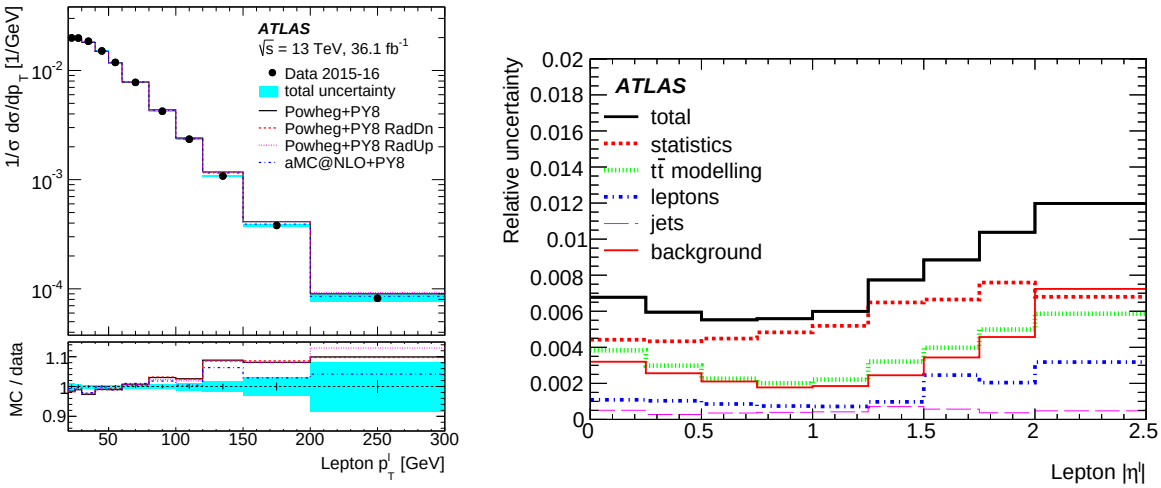

Figure 3: The normalized differential cross-section as a function of the lepton p_{T} (left). Relative uncertainties on the measured normalized differential cross-section as a function of the absolute value of the lepton pseudorapidity (right) [2].

tion of $t\bar{t}$ production and allowing the detailed search for a presence of BSM effects. The differential cross-sections are measured precisely in the dilepton channel as a function of various lepton variables and their combinations [2]. Figure 3 shows the normalized differential cross-section as a function of lepton p_{T} together with the relative uncertainties for the normalized differential cross-section as a function of the lepton pseudorapidity, where the uncertainties are typically below 1% level.

In the lepton+jets channel, many top quark and $t\bar{t}$ kinematic variables have been measured [6]. Figure 4 shows the examples of the measured distributions. Overall, the Monte Carlo (MC) generators, which include next-to-leading order (NLO) corrections, describe the kinematic distributions well, while there are some notable exceptions, e.g. the transverse momenta of top quarks and leptons are softer than the predictions, and $\Delta\phi$ between the leptons is shifted to lower values.

3 $t\bar{t}$ pair production with bosons and jets

The associated production of a top quark pair with bosons $(H, W^{\pm}, Z, \gamma)$ or jets is important due to various reasons, e.g. the $t\bar{t}$ + Higgs boson production allows us a direct measurement of the top quark Yukawa coupling while $t\bar{t} + b\bar{b}$ and $t\bar{t} + W/Z$ are very important background processes for $t\bar{t}$ + Higgs and many BSM searches, respectively.

The measurements of inclusive and differential $t\bar{t} + \gamma$ cross-sections have been performed in [7]. The fiducial cross-section is measured with a precision of about 6% and it is $\sigma = 44.2 \pm 0.9\ (\mathrm{stat.})^{+2.6}_{-2.4}\ (\mathrm{syst.})$ pb which is in an agreement with the NLO theory prediction $\sigma = 39.50^{+0.56}_{-2.18}\ (\mathrm{scale})^{+1.04}_{-1.18}\ (\mathrm{PDF})$ pb. Figure 5 shows the differential distribution as a function of photon p_{T}. Overall, there is a good agreement with the NLO predictions for the differential cross-sections.

The simultaneous inclusive measurement of the $t\bar{t}$ + Z boson and $t\bar{t}$ + W boson

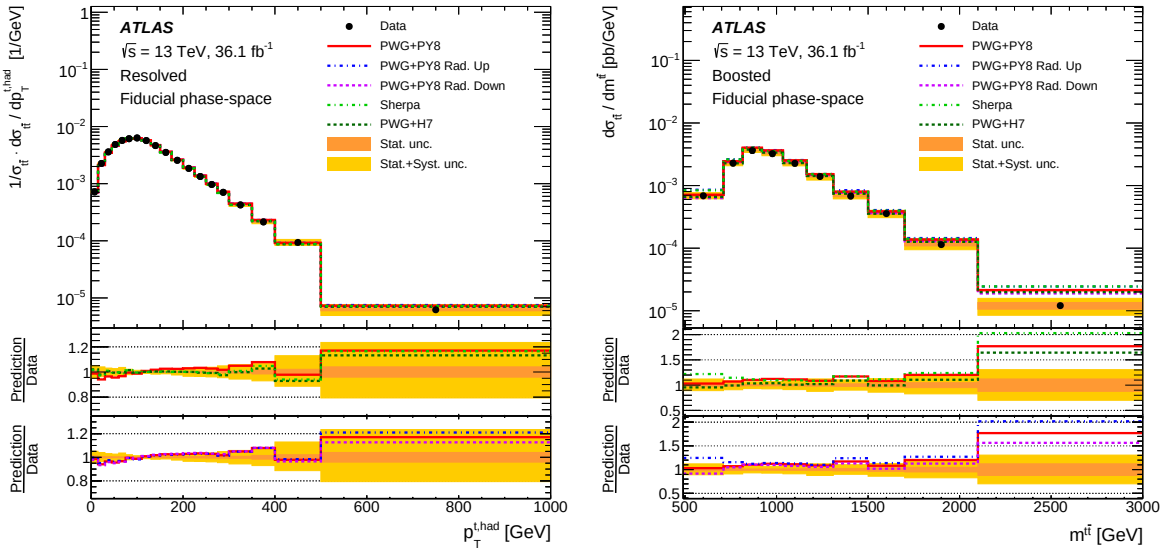

Figure 4: The normalized differential cross-section as a function of the transverse momentum of the hadronically decaying top quark (left) and the differential cross-section as a function of the $t\bar{t}$ invariant mass (right) [6].

cross-section has been performed using the yields in multilepton (2,3,4) final states [8], see Fig. 6 (left). The result of the fit is in a very good agreement with the SM prediction, as can be seen in Fig. 6 (right), while the relative precision of the measured cross-section is 13% and 22% for $t\bar{t} + Z$ and $t\bar{t} + W$, respectively.

The pair production of $t\bar{t} + b\bar{b}$ has a large theoretical uncertainty in the cross-section

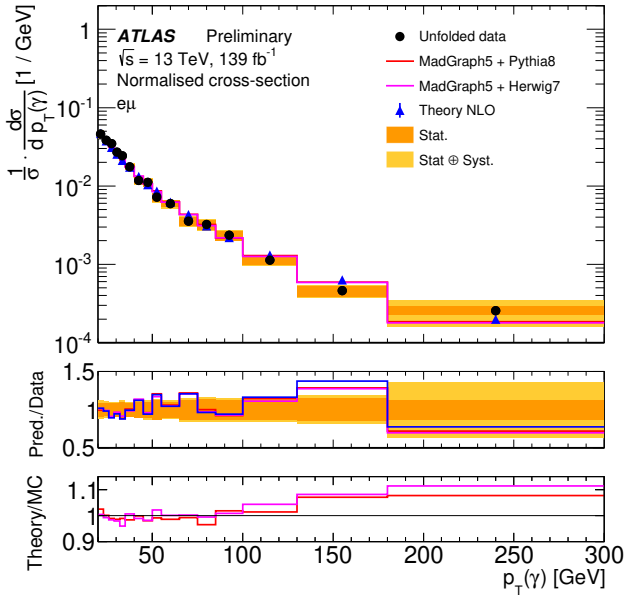

Figure 5: The normalized differential cross-section measured in the fiducial phase space as a function of the photon p_{T} [7].

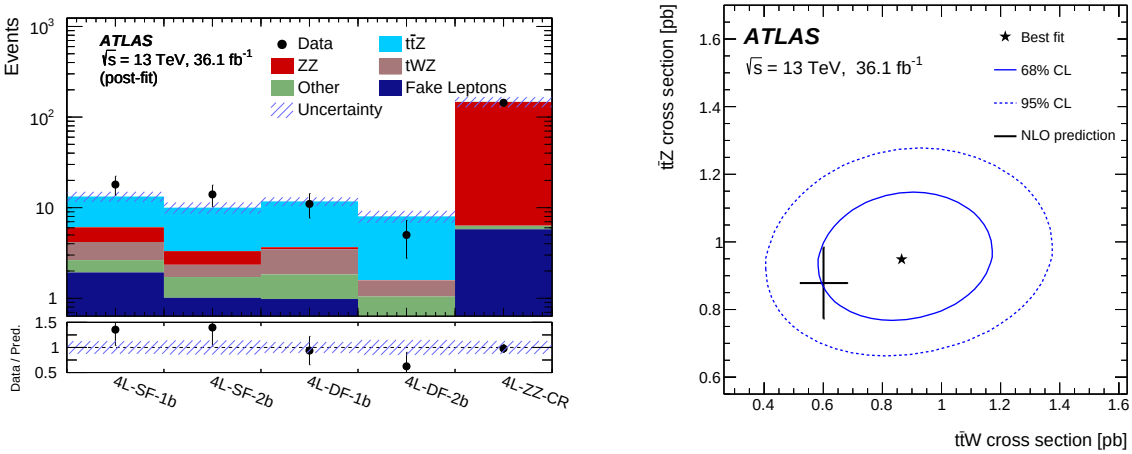

Figure 6: Event yields in data compared with the results of the fit in the tetralepton signal regions (left). The result of the simultaneous fit to the $t\bar{t} + Z$ boson and $t\bar{t} + W$ boson cross sections (right) [8].

prediction (25–30%) while being one of the most important background for the $t\bar{t} + H$ production. As seen in Fig. 7, the measured fiducial cross-sections in various final states are consistently higher, typically by 20-30%, than the predictions of various MC generators, while the normalized differential cross-sections are generally well described by MC predictions [9].

The $t\bar{t} + H$ process is being studied in many different Higgs decay channels. After the observation of $t\bar{t} + H$ where all major decay channels were combined [10], the goal is now to observe such a process in each individual decay mode. This was achieved recently with the $H \to \gamma\gamma$ decay mode with a significance of 4.9 standard deviations (s.d.) [11], see the diphoton mass spectrum in Fig. 8 (left). In the multileptons channel,

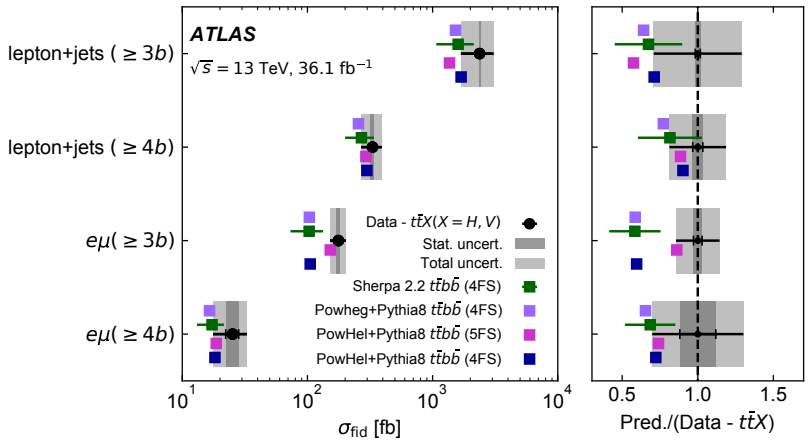

Figure 7: The measured fiducial cross-sections of $t\bar{t} + b\bar{b}$ in various decay channels compared with MC predictions [9].

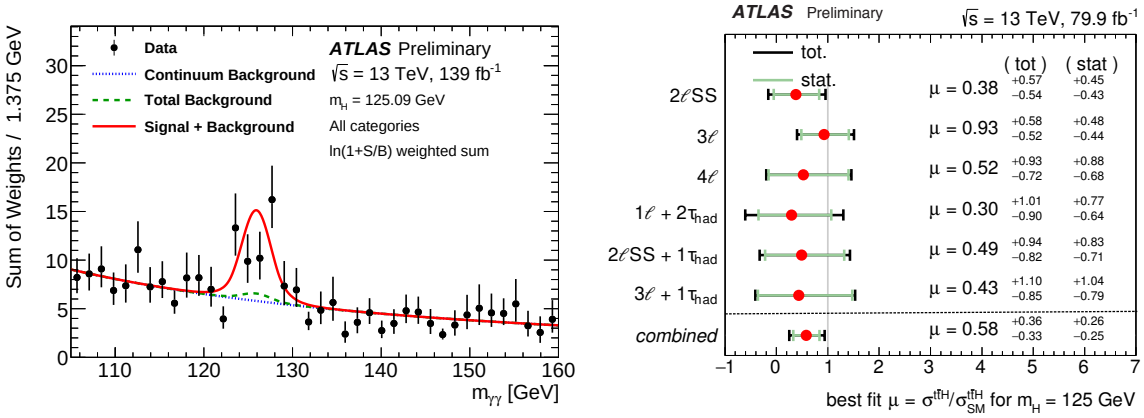

Figure 8: The weighted diphoton invariant mass spectrum for the sum of events in all categories (left) [11]. The observed best-fit values of the $t\bar{t}+H$ signal strength μ for each multilepton channel and combined (right) [12].

which includes $H \to WW/ZZ/\tau\tau$ processes, the overall significance is for now only at 1.8 s.d. (3.1 s.d. expected) [12]. Figure 8 (right) shows various decay channels used and their measured individual and combined signal strengths.

4 Flavour-changing neutral current searches

The flavour-changing neutral currents (FCNC) are extremely rare in the SM, so any observation of FCNC would mean the presence of BSM effects. Lately, ATLAS performed the searches involving the tqH and $tq\gamma$ vertex.

In the $tq\gamma$ analysis [13], both the production ($g+q \to q \to t+\gamma$) and the decay (e.g. $t\bar{t} \to q\gamma + Wb$) mode via FCNC are considered. The neural network (NN) is used to differentiate between events from the signal and background processes, see the NN output in Fig. 9 (left). The data are consistent with the background-only hypothesis. 95% CL upper limits are set on the branching ratio for the FCNC $t \to u\gamma$ decay via a left-handed (right-handed) $tu\gamma$ coupling of 2.8×10^{-5} (6.1×10^{-5}). Similarly, 95% CL upper limits are set on the branching ratio for the $t \to c\gamma$ decay via a left-handed (right-handed) $tc\gamma$ coupling of 22×10^{-5} (18×10^{-5}).

In the tqH search [14], two complementary analyses are performed to search for top-quark pair events in which one top quark decays into Wb and the other top quark decays into Hq, and target the $H \to b\bar{b}$ and $H \to \tau^+\tau^-$ decay modes, respectively. No significant excess of events above the background expectation is found. The combination with the previous searches in diphoton and multilepton final states yields 95% CL upper limits on the $t \to Hu$ and $t \to Hc$ branching ratio of 1.2×10^{-3} and 1.1×10^{-3}, respectively, see Fig. 9 (right).

All latest ATLAS and CMS FCNC searches are summarized in Fig. 10. No FCNC have been observed yet in the top quark sector. However, the measurements start to have the precision required to exclude at least some parts of particular BSM models.

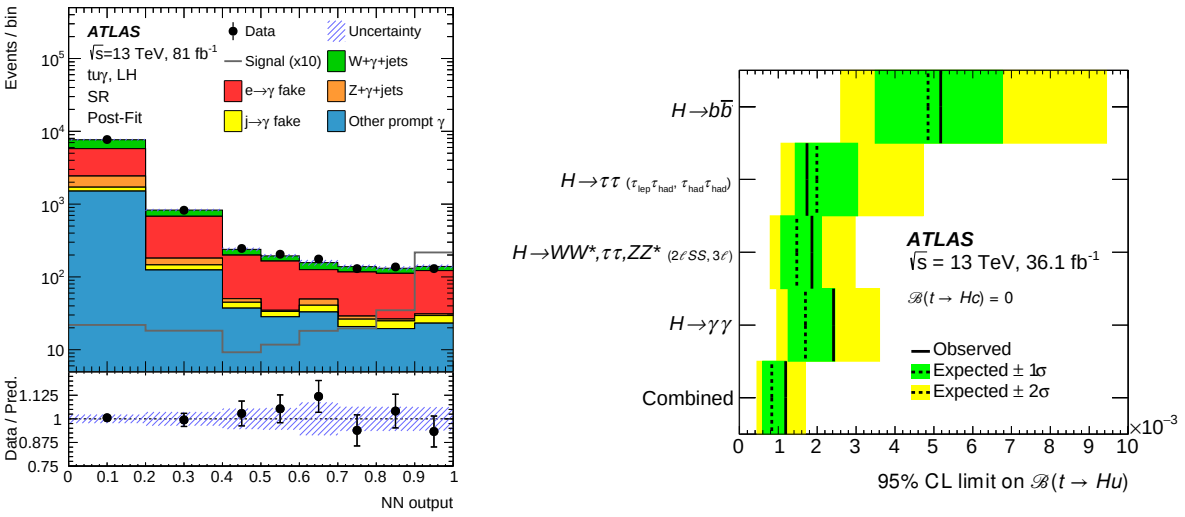

Figure 9: The post-fit neural network output distribution in the signal region (left) [13]. 95% CL upper limits on $B(t \to Hu)$ for the individual searches as well as their combination, assuming $B(t \to Hc) = 0$ (right) [14].

5 Top quark mass measurements

The top quark mass is probably the most important top quark parameter to be measured. It is a free parameter in the SM and many top quark predictions depend on its value. However, since the top quark is not a free particle and the precision of the measurements is increasing, the question of what we actually measure starts to become more and more important. Traditionally, the top quark mass has been measured by using the decay products of the top quark and comparing the data with the predictions from the MC generator, so called 'direct measurement'. This in fact measures the mass parameter in the MC generator. Does it correspond to the pole mass? This issue is still not completely solved. Therefore, the indirect measurements became more popular. Using the measured inclusive and differential cross-sections and the theoretical dependence of the cross-section on the top quark pole mass, it is possible to estimate it.

Two direct measurements of the top quark mass have been performed recently. One measurement was performed using the lepton+jets channel at the center-of-mass energy $\sqrt{s} = 8$ TeV. It uses the template 3-dimensional fit of the reconstructed top quark mass and variables which calibrate in-situ the jet and b-jet responses [16]. The measured top quark mass is 172.08 ± 0.39 (stat.) ± 0.82 (syst.) GeV. Combining this result with the best results in each other decay channel for both LHC Run 1 center-of-mass energies, $\sqrt{s} = 7$ TeV and $\sqrt{s} = 8$ TeV, the measured top quark mass is 172.69 ± 0.25 (stat.) $\pm$ 0.41 (syst.) GeV $= 172.69 \pm 0.48$ GeV($\pm 0.28\%$), see Fig. 11 (left).

The other direct measurement uses the invariant mass of the lepton and the soft p_{T} muon coming from the b-hadron decay [17], see Fig. 11 (right). The motivation for this method is to obtain the measurement which is insensitive to otherwise dominant jet related uncertainties. The measured top quark mass is 174.48 ± 0.40 (stat.) $\pm$ 0.67 (syst.) GeV $= 174.48 \pm 0.78$ GeV.

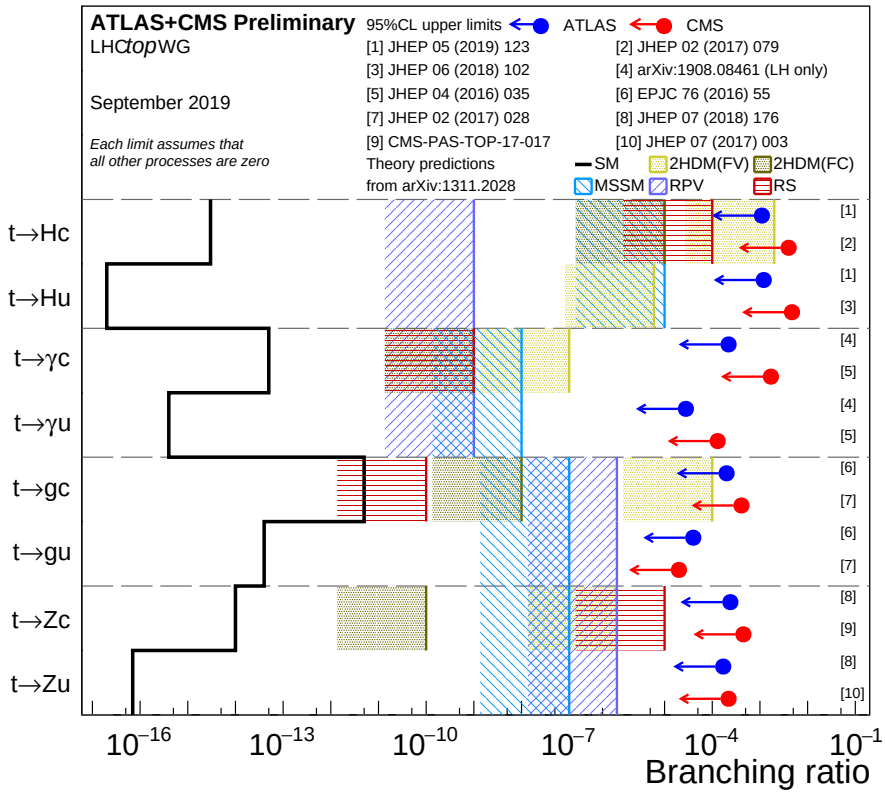

Figure 10: Summary of FCNC searches by the ATLAS and CMS Collaboration compared to several new physics models [15].

There are also two new indirect top quark mass measurements. First, the $t\bar{t}$ inclusive cross-section measurement in the dilepton channel has been used to measure the top quark pole mass using the theoretical $t\bar{t}$ cross-section dependence on the top quark pole mass [2], see Fig. 12 (left). The result is 173.1 ± 1.0 (exper.) $^{+1.5}_{-1.4}$ (PDF + α_s) $^{+1.0}_{-1.5}$ (scales) GeV. The other measurement was performed at $\sqrt{s} = 8$ TeV using $t\bar{t}$ + 1 jet events. It compares the normalized differential cross-section as a function of $\rho = 2m_0/m(t\bar{t}+1 \text{ jet})$, where m_0 is a constant fixed to 170 GeV, between the data and the theoretical prediction [18], see Fig. 12 (right). This allows us to decrease the theoretical uncertainty and the measured top quark pole mass is 171.1 ± 0.4 (stat.) ± 0.9 (syst.)$^{+0.7}_{-0.3}$ (theory) GeV. The summary of ATLAS and CMS indirect top quark pole mass measurements is presented in Fig. 13. The indirect top quark mass measurements seem to be consistent with the direct mass measurements at the current precision although the latest most precise top quark pole mass measurements point to a little bit lower top quark pole mass compared to the direct top quark mass measurements.

6 Top quark properties

A few measurements of the properties of the top quark production have been performed testing SM predictions in detail.

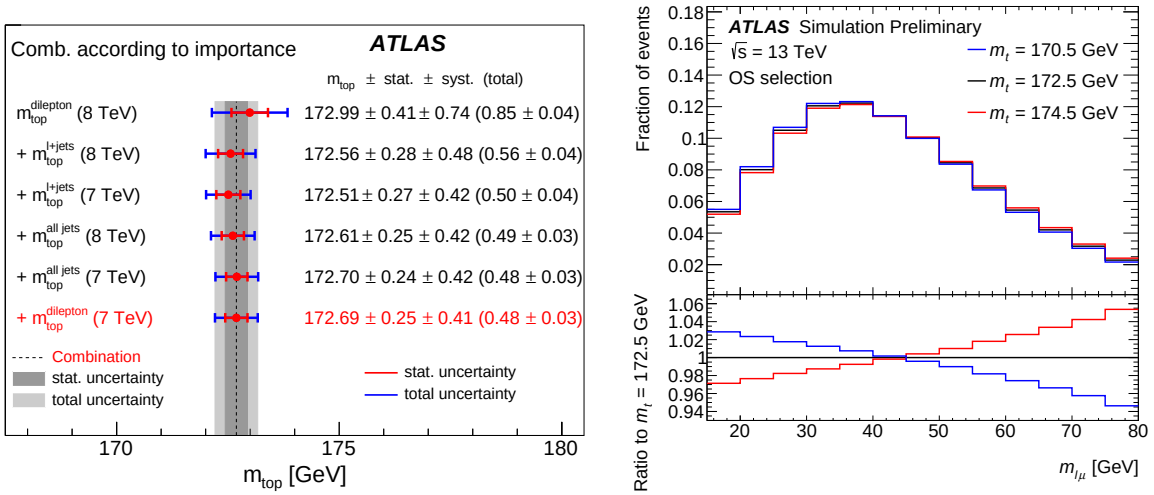

Figure 11: The result of the combination of direct top quark mass measurements from various channels when successively adding results to the most precise one (left) [16]. Sensitivity of the invariant mass of the lepton and the soft p_{T} muon to different input top quark mass (right) [17].

The charge asymmetry in the $t\bar{t}$ production is a small effect caused by higher order corrections. Such an effect could be enhanced by the presence of BSM processes. The ATLAS experiment measures the charge asymmetry $A_C = [N(\Delta|y| > 0) - N(\Delta|y| < 0)]/[N(\Delta|y| > 0) + N(\Delta|y| < 0)]$ using the number of events, N, with the opposite sign of $\Delta|y| = |y_t| - |y_{\bar{t}}|$ [20], see Fig. 14 (left). For the first time, the measured inclusive asymmetry $A_C = 0.0060 \pm 0.0015$ provides the evidence for non-zero charge asymmetry, at the level of 4 standard deviations. The result is consistent with the latest theoretical prediction $A_C = 0.0064 \pm 0.0005$. The asymmetry is measured also as a function of a

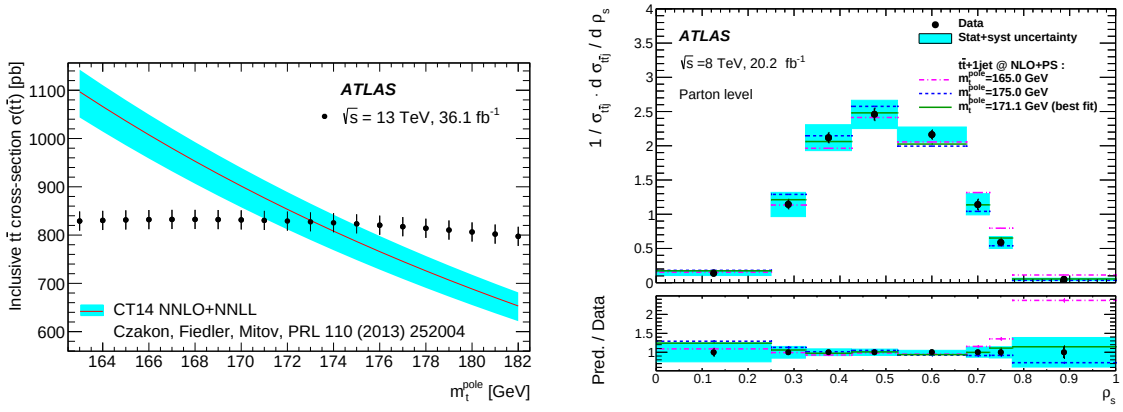

Figure 12: The predicted inclusive $t\bar{t}$ cross-section as a function of the top quark pole mass for the CT14 PDF set together with the experimental measurement and its dependence on the assumed value of top quark mass (left) [2]. The normalized differential cross-section for $pp \to t\bar{t}$ + jet production as a function of ρ (right) [18].

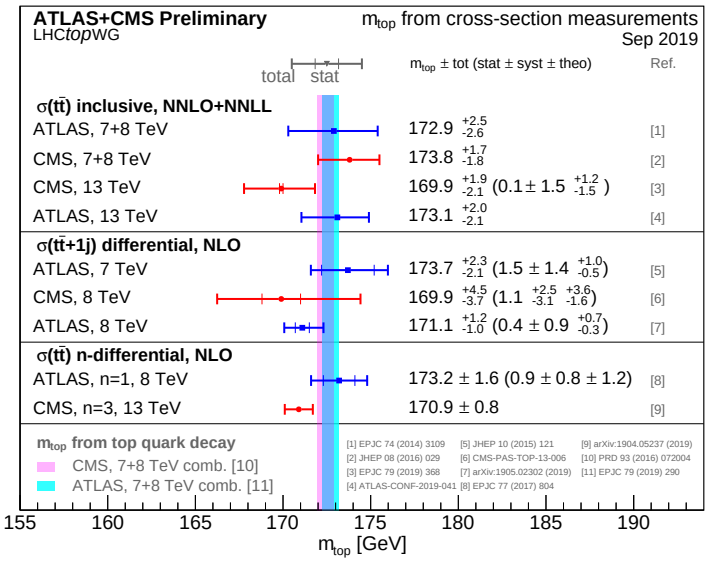

Figure 13: Summary of the ATLAS and CMS measurements of the top quark mass from $t\bar{t}$ production observables together with the combined direct ATLAS and CMS top quark mass measurements [19].

few kinematic variables, e.g. as a function of the invariant mass of the $t\bar{t}$ system, see Fig. 14 (right).

The direct measurement of the top quark width has been performed too [21]. The template fit is performed using the invariant mass of the lepton and the b-jet, see Fig. 15 (left). The measured width $1.94^{+0.52}_{-0.49}$ GeV is consistent with the SM prediction of 1.32 GeV.

Another measurement of top quark properties performed recently is the measurement of the spin correlations between the top quark and the antitop quark. Since the top quark

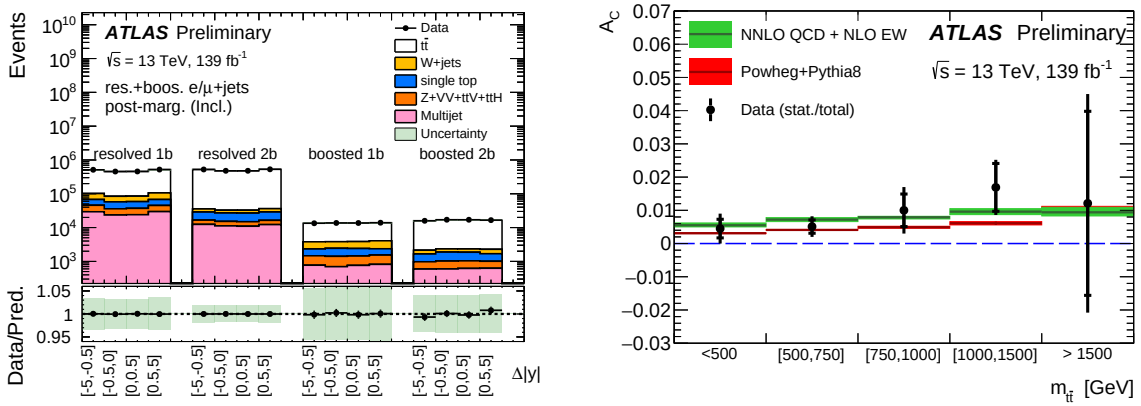

Figure 14: The comparison between the data and the prediction for rapidity bins corresponding to different signal regions used in the inclusive A_C measurement (left). The differential charge asymmetry as a function of the invariant mass of the top quark pair system (right) [20].

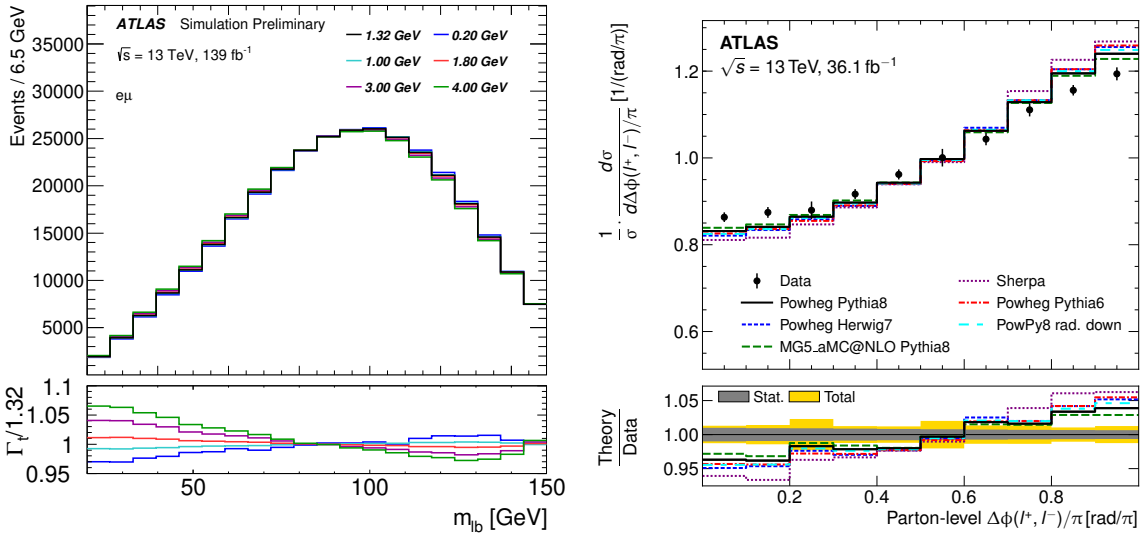

Figure 15: The $m_{\ell b}$ distribution for various top-quark decay widths (left) [21]. The normalized differential cross-section as a function of normalized $\Delta\phi$ between the leptons (right) [22].

has a very large width and consequently small lifetime, the top quark spin information is transferred and can be accessed through its decay products. The observable sensitive to the $t\bar{t}$ spin correlations is the polar angle between leptons $\Delta\phi(l^+, l^-)$, see Fig. 15 (right). The fraction of SM-like spin correlation is extracted to be $f_{SM} = 1.249 \pm 0.024$ (stat.) $\pm$ 0.061 (syst.) $\pm$ 0.040(theory) which is 3.2 standard deviations larger than the NLO prediction by the POWHEG MC generator ($f_{SM} = 1.0$) [22]. The latest theoretical prediction at NNLO suggests a smaller disagreement with the data although the deviation can not be fully explained by including just the higher-order calculation [23].

7 Summary

The ATLAS experiment produced lots of detailed and precise studies of the top quark during the last year. The inclusive cross-section has been measured with a precision of 2.4% in dilepton channel, while some normalized differential distributions of the leptonic observables have been measured with a precision better than 1%. The differential cross-sections are mostly well described by NLO predictions. The top quark pair events have been observed also with an association of bosons and jets. The top quark mass is measured with a precision of about 0.5 GeV, while the evidence for non-zero charge asymmetry has been measured. The top quark properties are mostly consistent with the Standard Model predictions. The only exception is the measurement of $t\bar{t}$ spin correlations where a deviation is seen at the level of 3.2σ, from the NLO MC prediction, while the deviation is lower when using the latest state-of-the-art NNLO prediction. No flavour-changing neutral currents have been observed yet.

References

[1] ATLAS Collaboration, JINST **3** (2008) S08003.

[2] ATLAS Collaboration, arXiv:1910.08819 [hep-ex].

[3] ATLAS Collaboration, ATLAS-CONF-2019-044, https://cds.cern.ch/record/2690717.

[4] M. Czakon and A. Mitov, Comput. Phys. Commun. **185** (2014) 2930, arXiv:1112.5675 [hep-ph].

[5] ATLAS and CMS Collaborations, JHEP **1905** (2019) 088, arXiv:1902.07158 [hep-ex].

[6] ATLAS Collaboration, arXiv:1908.07305 [hep-ex].

[7] ATLAS Collaboration, ATLAS-CONF-2019-042, http://cds.cern.ch/record/2690350.

[8] ATLAS Collaboration, Phys. Rev. D **99** (2019) no.7, 072009, arXiv:1901.03584 [hep-ex].

[9] ATLAS Collaboration, JHEP **1904** (2019) 046, arXiv:1811.12113 [hep-ex].

[10] ATLAS Collaboration, Phys. Lett. B **784** (2018) 173, arXiv:1806.00425 [hep-ex].

[11] ATLAS Collaboration, ATLAS-CONF-2019-004, https://cds.cern.ch/record/2668103.

[12] ATLAS Collaboration, ATLAS-CONF-2019-045, https://cds.cern.ch/record/2693930.

[13] ATLAS Collaboration, Phys. Lett. B **800** (2019) 135082, arXiv:1908.08461 [hep-ex].

[14] ATLAS Collaboration, JHEP **1905** (2019) 123, arXiv:1812.11568 [hep-ex].

[15] ATLAS Collaboration, ATL-PHYS-PUB-2019-038, https://cds.cern.ch/record/2691201.

[16] ATLAS Collaboration, Eur. Phys. J. C **79** (2019) no.4, 290, arXiv:1810.01772 [hep-ex].

[17] ATLAS Collaboration, ATLAS-CONF-2019-046, https://cds.cern.ch/record/2693954.

[18] ATLAS Collaboration, JHEP **1911** (2019) 150, arXiv:1905.02302 [hep-ex].

[19] ATLAS Collaboration, ATL-PHYS-PUB-2019-036, https://cds.cern.ch/record/2690526.

[20] ATLAS Collaboration, ATLAS-CONF-2019-026, http://cds.cern.ch/record/2682109.

[21] ATLAS Collaboration, ATLAS-CONF-2019-038, http://cds.cern.ch/record/2684952.

[22] ATLAS Collaboration, arXiv:1903.07570 [hep-ex].

[23] A. Behring, M. Czakon, A. Mitov, A. S. Papanastasiou and R. Poncelet, Phys. Rev. Lett. **123** (2019) no.8, 082001, arXiv:1901.05407 [hep-ph].